This is the accepted manuscript version of the contribution published as:

Wiltschka, K., Neumann, L., Werheid, M., Bunge, M., Düring, R.A., **Mackenzie, K.**, Böhm, L. (2020):
Hydrodechlorination of hexachlorobenzene in a miniaturized nano-Pd(0) reaction system combined with the simultaneous extraction of all dechlorination products
Appl. Catal. B-Environ. , art. 119100

The publisher's version is available at:

http://dx.doi.org/10.1016/j.apcatb.2020.119100

*Revised Manuscript
Click here to view linked References

Hydrodechlorination of hexachlorobenzene in a miniaturized nano-Pd(0) reaction system combined with the simultaneous extraction of all dechlorination products

Katrin Wiltschka[a], Larissa Neumann[a], Matthias Werheid[b,2], Michael Bunge[c,1], Rolf-Alexander Düring[a], Katrin Mackenzie[d], Leonard Böhm[a,]*

[a] Institute of Soil Science and Soil Conservation, Research Centre for BioSystems, Land Use and Nutrition (iFZ), Justus Liebig University Giessen, Heinrich-Buff-Ring 26-32, 35392 Giessen, Germany

[b] Physical Chemistry, Technical University Dresden, Bergstraße 66b, 01062 Dresden, Germany

[c] Institute of Applied Microbiology, Research Centre for BioSystems, Land Use and Nutrition (iFZ), Justus Liebig University Giessen, Heinrich-Buff-Ring 26-32, 35392 Giessen, Germany

[d] Helmholtz-Centre for Environmental Research – UFZ, Department of Environmental Engineering, Permoserstrasse 15, 04318 Leipzig, Germany

[1] Present address: Covestro Deutschland AG, 51373 Leverkusen, Germany

[2] Present address: Physical Chemistry, Carl von Ossietzky University of Oldenburg, 26129 Oldenburg, Germany

[*] Corresponding author: Leonard.Boehm@umwelt.uni-giessen.de

HIGHLIGHTS *(also submitted as separate file)*

- Miniaturized reactor system designed with simultaneous analyte extraction by SPME
- Pd(0) nanoparticles reduced HCB at environmental relevant concentrations
- Dechlorination pathways of all 12 chlorinated benzenes were elucidated
- Vicinal dechlorination pathway from hexachlorobenzene to benzene predominant

GRAPHICAL ABSTRACT *(also submitted as separate file)*

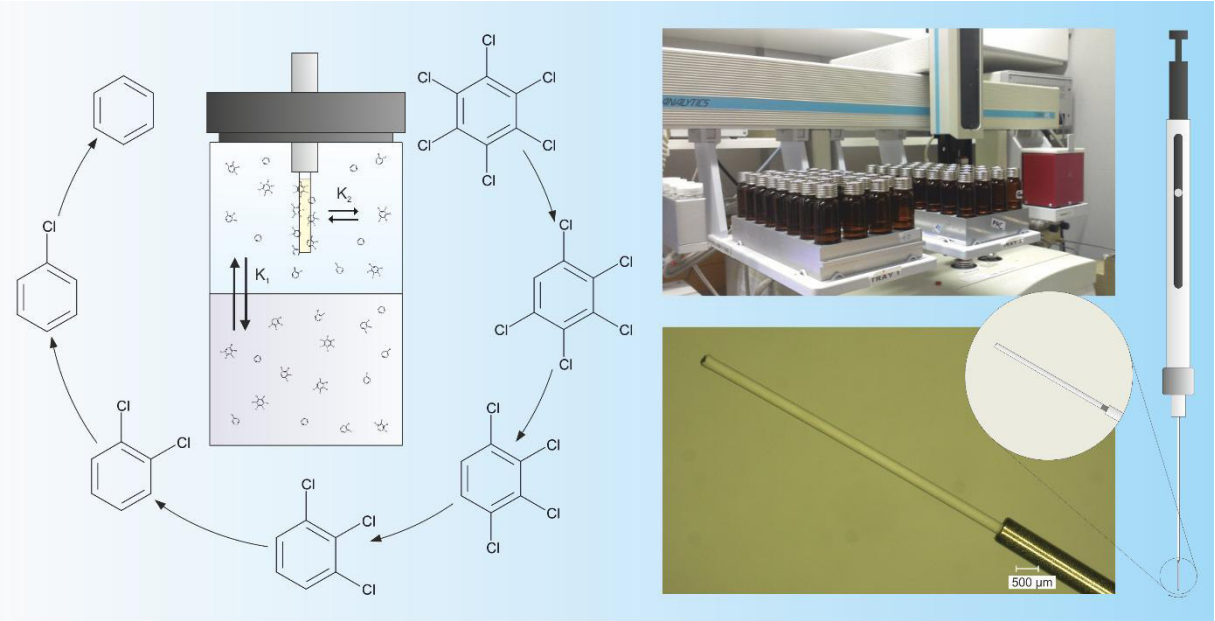

Abstract

The persistent organic pollutant hexachlorobenzene and all 11 further chlorobenzenes were hydrodechlorinated at environmentally relevant concentrations in miniaturized reaction systems, catalyzed by low concentrated Pd(0)-nanoparticles, to examine differences in dechlorination rates and pathways. Using solid-phase microextraction coupled to gas chromatography-mass spectrometry allowed the simultaneous extraction and detection of reactants, intermediate products and fully dechlorinated benzene, regardless of their different physicochemical properties. Dechlorination of HCB with formation of intermediates mainly proceeded via pentachlorobenzene, 1,2,3,4-tetrachlorobenzene, 1,2,3-trichlorobenzene, 1,2-dichlorobenzene, and monochlorobenzene to benzene. Specific catalytic activities of Pd(0)-nanoparticles (100–3400 L g^{-1} min^{-1}) differed depending on chlorination degree of chlorobenzenes and position of chlorine atoms. An inductive effect is assumed to favor a removal of the vicinal chlorine atom. The presented method permits the facile determination and comparison of nanomaterials' specific catalytic activities and allows the elucidation of dehalogenation pathways. It further enables to specifically examine formed intermediates to assess their toxicity and biodegradability.

Keywords

chlorobenzenes, transformation products, palladium (Pd) nanoparticles, specific catalytic activity, solid-phase microextraction (SPME)

Declaration of interest: none.

53 **1. Introduction**

54 Persistent organic pollutants (POPs) are characterized by long lifetimes in the environment,
55 possible long-range transport, a high potential for bioaccumulation and often also a negative
56 impact on human health and the environment [1]. Hexachlorobenzene (HCB) belongs to this
57 group of POPs and is part of the 'dirty dozen', initially 12 substances or substance groups that
58 are globally banned by the 2001 Stockholm Convention on POPs of the United Nations
59 Environment Program (UNEP) [2]. Furthermore, it is classified as persistent, bioaccumulative
60 and toxic (PBT) substance according to the European Union's chemicals legislation and is
61 suspected of being carcinogenic and teratogenic. It was used mainly as a fungicide or as
62 disinfectant in agriculture, but also as a wood preservative. Due to its persistency and despite the
63 global ban, HCB is still ubiquitous in the environment and consequently accumulates in food
64 webs [3]. In the environment, HCB can be degraded by photolysis and chemical reactions with
65 radicals [4], therefore methods based on irradiation for the degradation of chlorobenzenes are
66 constantly further developed [5,6]. Microbial degradation of HCB in soils and sediments mainly
67 occurs under anaerobic conditions, whereas less chlorinated compounds can be degraded also by
68 oxidation [7]. The pathways for microbial and photolytic dechlorination are very similar.
69 However, these degradation mechanisms occur in nature only to a limited extend, because
70 chemical reduction can require high energy input and biodegradation is not efficient enough. The
71 high catalytic activities of Pd nanoparticles indicate an enormous intrinsic potential for the
72 transformation of contaminants [8]. Supported by their large specific surface area, catalytically
73 active metal nanoparticles can be used to efficiently dechlorinate HCB and further halogenated
74 organic pollutants even under moderate conditions [9–11]. In these reactions, metal nanoparticles
75 catalyze the formation of activated hydrogen, which is able to perform the substitution of

76 halogen atoms in the POP molecule [12], while hydrochloric acid (HCl) in case of dechlorination
77 reactions is released. The presence of dissociated HX in higher concentrations in the near
78 vicinity of Pd can lead to self-poisoning of the catalyst material. Sufficient amounts of aqueous
79 solution or even addition of buffers offer a gradient for HX withdrawal from the active centers
80 [9]. Furthermore, Pd(0) nanoparticles are sensitive to poisoning by matrix constituents (e.g.,
81 salts). A further disadvantage is that suitable separation and recycling processes still have to be
82 developed [13]. Although the intrinsic activity of nanoparticles is mostly comparable to
83 supported catalysts, the minimized mass transfer in aqueous media when using nanoparticles is
84 beneficial. Catalysis promoted by Pd is seen as one of the most promising strategies to efficiently
85 remove reducible contaminants in water treatment approaches [14]. Highest reaction rates are
86 reached when using nanosized catalyst particles [9,15]. When applying nanosized catalysts, a
87 suitable suspending agent is needed in order to prevent agglomeration of the particles, and an
88 appropriate source of hydrogen. Hydrodehalogenation of higher halogenated substances using Pd
89 catalysts can generally lead to fully dehalogenated products. However, it seems that a direct
90 pathway, but also a successive stepwise dehalogenation pathway exist in parallel. If
91 dehalogenation is not complete, less halogenated intermediate products can remain. Generally,
92 they are recognized as less dangerous in the environment compared to the higher halogenated
93 substances, especially due to an easier microbial transformation, a lower bioaccumulation
94 potential and an often reduced toxicity [13]. However, specific transformation products can be
95 formed that are more toxic compared to others or the parent compound itself. This is most
96 obvious for the dechlorination of dioxins where formation of the highly toxic congener 2,3,7,8-
97 tetrachlorodibenzo-*p*-dioxin has to be avoided [16]. Another example of highly undesired
98 intermediates of a stepwise dechlorination is the formation of vinylchloride from polychlorinated

99 ethenes [17]. For the group of chlorobenzenes, toxicity also varies between its representatives.
100 Therefore, it is most helpful to know dehalogenation pathways in full detail. However, the
101 analytical monitoring of intermediate steps within the dehalogenation process can be very
102 laborious due to the highly varying characteristics of reactant, intermediate products, reaction
103 rates and the final dehalogenation product. This can require the combination of various
104 extraction methods, such as headspace extraction for (highly) volatile substances and solvent
105 extraction with filtration and concentration of solvent extracts. With solid-phase microextraction
106 (SPME), a technique is available that can facilitate the extraction of substances with varying
107 physicochemical properties, usually when using multiple extraction phases. SPME is a
108 solventless, miniaturized, equilibrium based, and mostly non-exhaustive extraction method,
109 which is built on the partitioning of analytes between the sample and a polymer-coated quartz
110 fiber that is introduced directly to the sample (immersed SPME) or to the headspace above the
111 sample (HS-SPME) [18–21]. Depending on the type of commercially available fibers, different
112 coating materials exist that provide targeted selectivity for matrix separation and the extraction
113 of analytes. Using an appropriately equipped autosampler, samples can be extracted
114 consecutively by the same fiber in an "agitator", a device which can be programmed to specific
115 stirring speed and extraction temperatures. After extraction, the fiber is transferred to the
116 injection system of the gas chromatography-mass spectrometry (GC-MS) instrument, where the
117 thermal desorption of analytes is performed before regular GC-MS analysis. Potential carry-over
118 of analytes by the fiber between samples can be avoided when a conditioning station is used in
119 which the fiber is additionally heated between sampling events. Quantification can be easily
120 performed with external standard calibration and internal standards. Besides saving solvents, the
121 use of SPME can significantly reduce labor time and allow extractions specific to individual

122 research questions. However, method development can be extensive, because several parameters
123 such as type of fiber coatings, extraction time, extraction temperature, stirring speed, and
124 conditioning of the fiber have to be investigated [19–22]. For HCB and its transformation
125 products as environmentally relevant target analytes an efficient monitoring in reaction
126 approaches and natural matrices is necessary. Therefore, the aims of this study were (i) to
127 establish a SPME method for the simultaneous extraction of HCB and all dechlorination
128 products directly from a miniaturized reaction system, (ii) to elucidate the dechlorination
129 pathways by tracking intermediate products and examining their dechlorination behavior, and
130 (iii) to determine the specific catalytic activity of Pd(0) nanoparticles for the dechlorination of
131 HCB and its transformation products. Hence, a SPME method was established for the
132 examination of HCB dechlorination in the presence of low concentrations of Pd(0) nanoparticles
133 in aqueous solution under anoxic conditions in a miniaturized reaction system with hydrogen as
134 reducing agent. Furthermore, the intermediate steps of the dechlorination of HCB to benzene
135 were investigated. HCB and all possible intermediates were used as individual reactants.

136

137 **2. Materials and methods**

138 *2.1 Chemicals and catalysts*

139 Molecular structures and physicochemical properties of the test substances HCB,
140 pentachlorobenzene (PeCB), tetrachlorobenzene (TeCB) isomers (1,2,3,4-TeCB, 1,2,3,5-TeCB,
141 and 1,2,4,5-TeCB), trichlorobenzene (TCB) isomers (1,2,3-TCB, 1,2,4-TCB, and 1,3,5-TCB),
142 dichlorobenzene (DCB) isomers (1,2-DCB, 1,3-DCB, and 1,4-DCB), monochlorobenzene
143 (MCB), and benzene (B) are summarized in Table S1 in the supporting information. All analytes

144 were purchased as neat substances from Dr. Ehrenstorfer GmbH (Augsburg, Germany) (purities
145 ≥ 98.0 %), prepared as stock solutions of single substances in methanol (123–1032 mg L^{-1}), and
146 mixed to concentrations of 0.05, 0.5, and 5 mg L^{-1} of each substance in methanol (methanol
147 purity ≥ 99.9 %, p.a. quality, Carl Roth GmbH, Karlsruhe, Germany) yielding working solutions
148 for calibration. Stock solutions of single substances were diluted in methanol to concentrations of
149 10 mg L^{-1} yielding working solutions for dechlorination experiments. Stock solutions in
150 methanol were stored in screw top vials with Mininert valves (CZT analytical equipment, Kriftel,
151 Germany), working solutions (10 mg L^{-1}) were stored in Certan capillary bottles (LGC Standards
152 GmbH, Wesel, Germany). For the internal standard mix, benzene-d_6 (2 mg L^{-1} in methanol, Dr.
153 Ehrenstorfer) was combined with a mixture of ^{13}C labeled mono- to hexachlorobenzenes (mono-
154 to-hexachlorobenzene solution [$^{13}C_6$, 99 %] 500 µg L^{-1} in toluene, CIL brand purchased from
155 LGC Standards, Wesel, Germany) and diluted in methanol (5 mg L^{-1}).

156 An aqueous working solution for dechlorination experiments was prepared with 9 g L^{-1} $NaHCO_3$
157 for pH stabilization (purity ≥ 99.5 %, p.a. quality, Carl Roth GmbH, Karlsruhe, Germany) [23]
158 and 2.94 g L^{-1} tri-sodium citrate dihydrate for nanoparticle stabilization (purity ≥ 99.0 %, p.a.
159 quality, Carl Roth GmbH, Karlsruhe, Germany) in a 1000-mL volumetric flask filled up with
160 water [9].

161 The Pd nanoparticles utilized in dechlorination experiments were obtained by chemical reduction
162 of the tetrachloropalladate complex with sodium borohydride as reducing agent [24]. Particles
163 were suspended in an aqueous solution (60 mg L^{-1}) containing citrate for stabilization purpose.
164 The final colloid suspension contained finely dispersed spherical Pd nanoparticles with an
165 average size of 3.9 nm (d50%; transmission electron microscopy, TEM) and was electrostatically
166 stabilized in a pH range of 8 to 9 (Figure S1). Immediately before the start of the experiment, the

167 suspension was transferred via air cushion pipette into 20-mL vials and gassed with hydrogen for
168 30 min for the activation of the catalyst material [9].

169 A solution of sodium sulfite (Na_2SO_3) (purity ≥ 98.0 %, p.a. quality, Carl Roth, Karlsruhe,
170 Germany) was produced in a concentration of 60 g L^{-1} in water, ensuring a 5-fold stoichiometric
171 excess when added to end dechlorination reactions by catalyst poisoning.

172 All water used within the study was of ultrapure quality (Milli-Q Advantage A10 System,
173 Millipore).

174

175 *2.2 Preparation and design of experiments*

176 The stabilization solution and nano-Pd suspension were flushed with hydrogen for 30 min. The
177 containers were hermetically sealed by membranes (silicone / PTFE). The pure hydrogen was
178 introduced with a sterile disposable needle (Sterican, Braun Melsungen AG, Melsungen,
179 Germany). In order to prevent a potential contamination with particles or oil residues from the
180 gas supply line, a syringe filter (Filtropur S 0.2, Sarstedt, Nümbrecht, Germany) was placed in
181 line. Another sterile needle ensured that the previously contained air composition could escape.
182 The resulting holes served later as a puncture site for the microliter glass syringe.

183 Dechlorination experiments described below were performed in an anaerobic chamber
184 (glovebox, Mecaplex, Grenchen, Switzerland) with N_2/CO_2 atmosphere (ratio 80:20, "Foodpack
185 3", Praxair, Germany), to provide anoxic conditions for reductive dechlorination experiments.

186 9.95 mL of the $NaHCO_3$ solution and 50 µL nano-Pd suspension were filled in 20-mL amber
187 glass vials yielding an experimental concentration of 300 µg Pd L^{-1}. Vials were sealed with

188 magnetic screw caps with PTFE septa for use with the autosampler (CS-Chromatographie
189 Service GmbH, Langerwehe, Germany). Using a syringe, 1 mL of the gas phase was withdrawn
190 and replaced with 1 mL hydrogen to provide a concentration of 10 % hydrogen (v/v) in the
191 N_2/CO_2 atmosphere of the samples. Through the remaining hole, the samples were each spiked
192 with 3 µL HCB solution (or 3 µL of PeCB, 1,2,3,5-TeCB, 1,2,4,5-TeCB, 1,2,3,4-TeCB, 1,3,5-
193 TCB, 1,2,4-TCB, 1,2,3-TCB; or 6 µL of 1,4-DCB, 1,3-DCB, 1,2-DCB, MCB solution, each
194 10 mg L^{-1}). An automated glass microliter syringe (eVol® Dispensing System, Thermo Fisher
195 Scientific) was used for spiking to achieve a final concentration of 3 µg L^{-1} (or 6 µg L^{-1}) for the
196 above listed reactants. After HCB was added to the Pd suspension, the system was shaken
197 continuously at 300 rpm on a horizontal shaker (VWR International) throughout the reaction
198 ensuring sufficient contact and distribution of reactants, nanocatalysts and hydrogen. All
199 reactions were performed at room temperature (22±1 °C). The dechlorination reaction was
200 stopped after 1, 3, 6, 12, 30, and 60 min by adding 10 µL of a 60 g L^{-1} Na_2SO_3 solution as
201 catalyst poison to the sample. Subsequently, 2 µL of internal standard solution was injected
202 through the septa and the syringe holes in the caps were sealed with superglue (Ultra Gel, Pattex,
203 Henkel, Düsseldorf, Germany). Samples were prepared in four replicates for each of the 6
204 reaction times.

205 Calibration samples were prepared in Pd solution to avoid matrix differences between calibration
206 samples and dechlorination samples. Calibration samples were prepared in duplicates for a 7-
207 point calibration of benzene and chlorobenzenes (0.01–3 µg L^{-1}). Reference samples
208 (dechlorination time t = 0 min) were prepared with four replicates. In order to prevent
209 dechlorination in calibration and reference samples, Na_2SO_3 was added to the Pd suspension
210 before it was spiked with analytes (calibration or rather reactant solutions) and internal standards.

211 All other steps were kept constant to the procedure described above. Additionally, duplicate
212 blank samples were measured for the various media used (vials with 10 mL water, with 10 mL
213 $NaHCO_3$ solution containing 10 µL Na_2SO_3, and with 9.95 mL $NaHCO_3$ solution containing 50
214 µL nano-Pd suspension and 10 µL Na_2SO_3). After the experiments, the samples were exported
215 from the glovebox just before the measurement.

216

217 *2.3 Instrumental analysis*

218 Method development of the combined SPME-GC-MS method included optimization of SPME
219 extraction based on previous work by Böhm et al. [21,22], i.e. the parameters fiber coating,
220 extraction temperature, extraction time, thermodesorption temperature, as well as fiber cleaning
221 time and temperature were modified with regard to the different physicochemical properties of
222 benzene and the 12 chlorobenzenes. Simultaneous extraction of benzene and all chlorobenzenes
223 was tested with five different fiber coatings or fiber types (Supelco, Sigma-Aldrich): 100 µm
224 polydimethylsiloxane (PDMS); 65 µm mixed phase of divinylbenzene and PDMS (DVB/PDMS)
225 as both StableFlex and fused silica fiber; 85 µm polyacrylate (PA); and 50/30 µm mixed phase of
226 DVB, Carboxen and PDMS (DVB/CAR/PDMS). The GC method was optimized for a 60 m
227 column with regard to a baseline separation of the two isomers 1,2,3,5-TeCB and 1,2,4,5-TeCB,
228 which are often given as sum parameter in literature due to their similar chromatographic
229 retention [25,26]. The following procedure gives the optimized conditions: Samples were
230 extracted by automated HS-SPME on a CombiPAL autosampler (CTC-Analytics, Zwingen,
231 Switzerland) equipped with a combined heating/shaking device ("agitator") and a separate fiber
232 desorption oven ("needle heater") for the cleaning of SPME fibers between sampling events.

233 Extraction was performed with a 65 µm fused silica fiber with DVB/PDMS coating
234 (Supelco/Sigma-Aldrich 57345-U) for 20 min at 40 °C while shaking the sample at 250 rpm in
235 the agitator. Prior to extraction, samples were left in the agitator for 5 min at 250 rpm to allow
236 for an adaption to the extraction temperature by shaking and heating of the sample. After
237 extraction, the fiber was directly transferred to the injector of the GC-MS system, where it was
238 thermally desorbed for 3 min at 210 °C using a 1 mm SPME liner (Straight Inlet Liner, Restek,
239 Bad Homburg, Germany) in splitless mode. Detailed parameters for GC-MS conditions as well
240 as further procedures for quality assurance and quality control are given in Tables S2 and S3.

241

242 *2.4 Data analysis*

243 Raw data from GC-MS were processed with the software 'Xcalibur' (Thermo Fisher Scientific)
244 combined with a manual verification of peak integration. Data for all analytes were corrected
245 based on internal standards. The three isomers of DCB, TCB, and TeCB were corrected with one
246 internal standard per degree of chlorination (Table S2). Quantification was performed by
247 calibration with external standards. The four replicates per preset dechlorination time are given
248 as mean value. Standard deviation of the mean value was calculated as the square root of the
249 residual sum of squares divided by n with n as the number of replicates.

250

251 *2.5 Calculation of specific Pd activity for catalytic hydrodechlorination*

252 Empiric basis shows that the catalytic hydrodehalogenation of organic halogen compounds
253 follows 'pseudo first-order' kinetics with respect to reactants. The specific Pd activity of the

254 nanocatalyst in a dechlorination experiment with the substance 'i' ($A_{Pd,i}$) was calculated using the
255 following equation [27]:

$$A_{Pd,i}[\mathrm{L\,g^{-1}\,min^{-1}}] = \frac{V_{water}}{m_{Pd} \cdot \tau_{1/2}} = \frac{\ln\left(\frac{c_{t0,i}}{c_{tx,i}}\right)}{\ln 2 \cdot c_{Pd} \cdot (t_x - t_0)} \quad (1)$$

256 giving the water volume (V_{water} in [L]) contaminated with the substance '*i*' in a given
257 concentration $c_{t0,i}$, which can be treated with the mass of catalyst applied (m_{Pd} in [g]) yielding a
258 half-life of the reactant ($\tau_{1/2}$ in [min]); or rather with the concentration of the reactant ($c_{t0,i}$) and
259 ($c_{tx,i}$) at the chosen start time (t_0) and end time (t_x) (where x is the specific time of catalyst
260 poisoning, 1–60 min) of the dechlorination experiment, and the concentration of the catalyst
261 applied (c_{Pd}). For reaching a given elimination goal, $A_{Pd,i}$ therewith allows to calculate how much
262 Pd would be necessary to treat a certain volume of water in a certain time frame [13].

263

264 ## *3.* Results and discussion

265 ### *3.1 Simultaneous extraction of analytes by SPME*

266 The SPME fibers tested for the simultaneous extraction of HCB and all possible dechlorination
267 products widely differed in their sensitivity depending on the physicochemical characteristics of
268 the analytes. For the most commonly used SPME fiber (PDMS 100 µm), the amount of extracted
269 benzene was not sufficient. This was the same for the 85 µm PA fiber, which is often used for
270 more polar compounds. The DVB/CAR/PDMS fiber was very promising because the CAR phase
271 led to a very sensitive extraction of benzene, MCB and DCBs. However, thermal desorption
272 from the fiber was not sufficient for the higher chlorinated benzenes. This caused a carry-over
273 effect that could not be eliminated by an increase in thermodesorption temperature or increased

274 cleaning time in the needle heater. The amount of extracted benzene was much lower for the
275 DVB/PDMS fiber, but was sufficient for a valid detection at low benzene concentrations (linear
276 calibration curve down to 0.01 µg L^{-1}). Choosing a thermodesorption temperature (210 °C)
277 significantly lower than the maximum operating temperature given by the manufacturer (270 °C)
278 was crucial, since higher temperatures led to a slow but noticeable degradation of the DVB phase
279 resulting in interferences with the detection of benzene. These interferences could be avoided at
280 210 °C, while ensuring sufficient thermal desorption of HCB.

281 Simultaneous extraction of HCB and all possible dechlorination products made it possible to
282 follow the dechlorination reaction in terms of reactant reduction, appearance and disappearance
283 of intermediate products, and formation of the final product benzene as a function of time and
284 nanoparticle concentration. Therefore, dechlorination pathways could be derived.

285

286 *3.2 Dechlorination of chlorobenzenes by Pd nanocatalysts*

287 Hydrodechlorination of HCB and all further chlorobenzenes, as well as the formation of
288 intermediate products and benzene as the fully dechlorinated product were followed over time
289 (Figure 1). The individual intermediates of the dechlorination of HCB are shown in Figure 2
290 including the differentiation between isomers formed. For all dechlorination experiments, the
291 rate constant *k* value of pseudo first order kinetics for the disappearance of the reactant was
292 calculated (Figure S2). Figure 1 shows that the elimination of chlorobenzenes normally increases
293 with decreasing chlorination degree. Nonetheless, intermediate products were detected, as Figure
294 2 illustrates in more detail for HCB as parent compound. Slower abreaction of lower chlorinated
295 intermediates that were expected to react more quickly than the higher chlorinated species is not

296 fully understood and needs explanation. Figure 1 also shows that in some cases benzene
297 formation curves indicate a lag phase in the beginning, as for HCB itself, 1,2,4,5-TeCB and
298 1,2,4-TCB. In these cases, also the further reduction of intermediates seems slightly inhibited.
299 Stepwise reduction of chlorobenzenes seems dominant while direct dechlorination to benzene or
300 other less chlorinated chlorobenzenes in a single step, without detachment from the catalyst,
301 cannot be ruled out as parallel reaction. However, the product pattern found during
302 dechlorination suggests also preferred reaction pathways. Since benzene formation occurs for
303 most reactants immediately after the reaction start, not only the consecutive pathway can be
304 assumed, but in addition a multiplet mechanism as assumed by other studies [28-30]. For the
305 dechlorination of POPs, electron transfer mode [31] and hydrogen transfer mode [32] are seen as
306 the main dechlorination mechanisms. The latter mechanism is assumed to dominate in our
307 experiments because Pd(0)-generated activated hydrogen is present in the system and
308 consequently activated hydrogen is added electrophilically to the aromatic ring [33]. For
309 adsorbed polychloroaromatic compounds, the interaction between the lone electron pairs of the
310 chlorine atom and the π–cloud of the aromatic ring is discussed in such a way that the C-Cl bond
311 reaches the character of a double bond [29] leading to the elimination of several chlorine atoms
312 without desorption of the chloroaromatic substrate from the catalyst surface. The catalytic
313 hydrodechlorination is accelerated by the electron-withdrawing substituents stabilizing this
314 formal C=Cl double bond by withdrawing the electron density of the aromatic ring [30]. The
315 C=Cl bond becomes more pronounced the more chlorine atoms are present in the ring. The
316 electrons of chlorine and the aromatic ring are partially withdrawn from *d*-orbitals of the
317 transition metal (Pd). This is assumed to cause additional stabilization, allowing the formation of
318 two C=Cl bonds and the removal of two chlorine atoms without desorption of the chlorinated

319 benzene from the catalyst surface [28]. It is unclear why in the HCB reaction the intermediates
320 are existent for a longer time, whereas e.g. in the PeCB reaction, the dechlorination rate of the
321 formed intermediates is higher. This may indicate that the catalyst is affected by HCB in a
322 different way than in the presence of PeCB. It is possible that HCB is strongly stabilized in its
323 adsorption so that competitors cannot replace it until most of the HCB is dechlorinated.
324 Furthermore, faster reacting compounds such as DCBs should not or only minimally emerge in
325 these experiments. If the intermediates remain adsorbed on the catalyst surface during
326 dechlorination [28], and the C-Cl bonds are split one after the other, the intermediates only
327 appear when the system is disturbed and therefore are able to desorb (e.g., by Na_2SO_3 as catalyst
328 poison that reduces H_2 uptake of the catalyst and also modifies the catalyst surface by formation
329 of PdS). Because number and positions of chlorine substituents and therewith electronic effects
330 vary, chlorobenzenes can differ in their adsorption/desorption behavior on the catalyst surface,
331 which could influence the amount of detected analytes and therewith interpretation of
332 dechlorination pathways. However, these differences are taken into account by the use of internal
333 standards, which allow the correction for influences of sorption on the amount of detected
334 analytes. Although, based on the internal standards used, small deviations could occur for the
335 isomers with the same chlorination degree, these differences are seen to be negligible [21]. Based
336 on the experiments with the less chlorinated benzenes introduced as starting material, it was
337 possible to identify the quantitatively most abundant intermediates formed in the individual
338 dechlorination reactions. For the dechlorination of HCB to benzene, the intermediate products
339 PeCB and mainly the isomers 1,2,3,4-TeCB, 1,2,3-TCB, and 1,2-DCB were detected, suggesting
340 an attack of activated hydrogen on the vicinal chlorine atoms. When these intermediates were
341 introduced as starting reactant, the same pattern was obtained. In addition, MCB could be

342 detected as the last intermediate product of full dechlorination. Comparative dechlorination of all
343 TeCB, TCB, and DCB isomers revealed that the most abundant isomers are those with the
344 highest dechlorination rates as individuals. Instead of a relative enrichment of the non-vicinal
345 chlorinated isomers which are slower dechlorinated, lower concentrations of these substances as
346 intermediates were found. Consequently, this indicates that the vicinal chlorinated intermediates
347 are representative for a vicinal dechlorination pathway. Based on these dechlorination
348 experiments, the main gradational reaction pathways for the dechlorination of HCB using Pd(0)
349 nanoparticles are proposed, of which the progressive vicinal substitution of Cl is the dominating
350 hydrodechlorination route (Figure 3).

351 This represents a fundamentally different reaction pathway than has been demonstrated in
352 photolytic dechlorination (radical attack) [6] or microbiological dechlorination (reductive
353 dechlorination) [7,34], where 1,2,3,4-TeCB, 1,2,3-TCB and 1,2-DCB were not formed at all or
354 only in very small quantities. However, this is not unexpected, since these are different
355 mechanisms that bring different reaction patterns. In addition, considering the Gibbs free energy
356 values for the reductive dechlorination of chlorobenzenes, 1,2,3,4-TeCB, 1,2,3-TCB, and 1,2-
357 DCB are the energetically unfavorable intermediate products [35], but these isomers are found as
358 the relevant intermediate products within the present study. Surprisingly, the consecutive
359 mechanism part of hydrodechlorination by Pd(0) is identical to the mechanochemical
360 dechlorination by Mg/Al_2O_3 [36]. Non-hydrogenation active metals are another system with a
361 different mechanism (single electron transfer), which makes it difficult to accomplish the
362 aromatics dependent two-electron transition. Nevertheless, the mechanochemical reaction takes
363 place, possibly due to the increased energy input in mechanochemical reactions [37].

364 Based on a statistical distribution of randomly attacked chlorine atoms, the formation of specific
365 TeCB, TCB and DCB isomers is more likely. For example, assuming a dechlorination of PeCB
366 by chance, the formation of 1,2,4,5-TeCB is less probable (20 %) since specifically the 3-chloro
367 position of PeCB has to be substituted by hydrogen, whereas the formation of the two further
368 TeCB isomers is equally likely (40 % each) because a substitution of the 1-chloro and 5-chloro
369 or rather of the 2-chloro and the 4-chloro positions yield identical molecules, respectively.
370 Similar differences exist as well for the formation of TCB and DCB isomers. However, actual
371 occurrence and concentrations of isomers do not match a dechlorination by chance. Instead, the
372 formation is interpreted with regard to energetically beneficial reactions. It is claimed that the
373 transition states of PeCB, where the negative charge is on the carbon atom attached to the
374 hydrogen atom, are the most stable resonance structures that appear in different positions relative
375 to the hydrogen atom during the formation of the C=Cl bond [28]. In all other structures, the
376 negative charge is located at the carbon atom bound to the negatively charged chlorine atom.
377 Therefore, the formation of 1,2,3,5-TeCB, 1,3,5-TCB, and 1,3-DCB should be unlikely. This
378 partially contradicts the data presented in the present study, where the formation of 1,2,3,5-TeCB
379 was more comprehensive than the formation of 1,2,4,5-TeCB. One reason for this could be the
380 addition of a catalyst poison to terminate dechlorination reactions that could influence the
381 transition state at the decisive moment. However, other factors may also control the formation of
382 specific intermediates, such as unfavorable steric conditions and their partial charges. They could
383 serve as a “shielding wall”, promoting an inductive effect, which protects against dechlorination
384 attacks. The partial charges can further explain the slower dechlorination of HCB compared to
385 the less chlorinated benzenes (Figure 1), and the different formation of TeCBs with the
386 preference for 1,2,3,4-TeCB, a minor proportion of 1,2,3,5-TeCB, and a negligible formation of

387 1,2,4,5-TeCB. Since a chlorine atom is already substituted by hydrogen as in PeCB, the vicinal
388 chlorine atom is next to be replaced due to a lower inductive effect. Both TeCBs have
389 comparatively large gaps in their shielding wall, whereas for 1,2,4,5-TeCB the remaining
390 chlorine atoms are distributed in such a way that the smallest possible attack surface is formed.
391 The same applies more or less to the TCBs. The lack of three adjacent chlorine atoms in
392 1,2,3-TCB and two adjacent chlorine atoms in 1,2,4-TCB create a better contact surface (Figure
393 4).

394 However, in addition to inductive effects, also the affinity of the reactants for adsorption to the
395 catalyst has to be considered as influencing factor. Comparative studies on dechlorination
396 reactions of PCB 21 catalyzed by nanoparticles show that the chlorine atoms that are para to the
397 phenyl group are the ones first dechlorinated [38]. Further, it was shown for the dechlorination of
398 1,2,3,4-tetrachlorodibenzo-*p*-dioxin (TCDD) that the vicinal chlorine atom is preferably
399 substituted and the formation of 2,3-substituted congeners could not be detected [16,39]. In
400 contrast, in a catalyzed dechlorination using zinc nanoparticles, the vicinal chlorosubstituents of
401 octachlorodibenzo-*p*-dioxin are not split off, and thus no 2,3,7,8-TCDD is formed [40]. This
402 reinforces the assumption that different metal nanoparticles also induce different dechlorination
403 steps. So far, it seems that Pd(0) nanoparticles preferably induce a dechlorination of the vicinal
404 positioned chlorine, regardless of the chlorinated hydrocarbon reactant.

405 Test concentrations (3 µg L^{-1} for HCB, PeCB, TeCBs, TCBs, and 6 µg L^{-1} for DCBs and MCB)
406 reflect environmentally relevant concentrations for the low water-soluble hydrophobic
407 compounds. Commonly, dehalogenation of water pollutants means detoxification. Although, in
408 terms of acute toxicity, the LC50 for fish can be higher for some intermediates compared to
409 HCB. However, the persistent and bioaccumulative properties of HCB have to be taken into

410 account as well. For organisms in the aquatic environment and human health, it is nevertheless
411 regarded as beneficial when chlorobenzenes are dechlorinated because benzene and chlorinated
412 benzenes with low substitution degree have a much better biodegradability compared to HCB
413 [13,41]. The overall elimination rate of chlorinated benzenes and benzene in the environment is
414 therefore accelerated. Toxicity can vary widely among isomers with the same degree of
415 chlorination. While for the chlorobenzene isomers the differences in toxicity are comparatively
416 small, the presented approach is nevertheless promising to investigate and predict the formation
417 of highly toxic isomers after adaption of the method to further substances or substance groups.
418 Regarding this, it is relevant to elucidate if further halogenated pollutants are primarily degraded
419 by a vicinal dehalogenation pathway such as found for HCB, especially for the POPs where
420 specific isomers show highly varying toxicity, persistence, bioaccumulation potential, and long
421 range transport, e.g. polychlorinated dioxins and furans (PCDD/Fs), dioxin-like PCBs, or per-
422 and polyfluorinated or -brominated compounds. The corresponding C-X bond strengths in
423 halogenated hydrocarbons have been listed based on various studies [27]. For halobenzenes
424 (iodobenzene, bromobenzene, chlorobenzene, and fluorobenzene) comparison works well due to
425 the same structure and variation of the halogen substituent. With increasing electronegativity of
426 the halogen, the C-X bond has an increased strength and correspondingly a lower specific
427 catalyst activity results for hydrodehalogenation. Therefore, it can be assumed that
428 hexaiodobenzene, hexabromobenzene, and hexafluorobenzene will be dehalogenated via both
429 stepwise and multiplet mechanism just like HCB, except that the specific catalytic activity of Pd
430 nanoparticles would most likely be lower for hexafluorobenzene and higher for hexaiodobenzene
431 and hexabromobenzene. However, for larger substituents, such as bromine, the steric effects
432 might have an increased influence, as well as their adsorption to the catalyst surface.

433

434 *3.3 Catalytic activity of Pd nanocatalysts*

435 The catalytic Pd activities for chlorobenzenes, calculated according to equ. 1, are listed in
436 Table 1.

437 *Table 1. Specific catalytic activity of Pd(0) nanoparticles for the dechlorination of all*
438 *chlorobenzenes (d50% = 3.9 nm, $c_{0,CBs}$ = 3 µg L^{-1}, c_{Pd} = 300 µg L^{-1}, c_{NaHCO3} = 9 g L^{-1},*
439 *$c_{Na\text{-}citrate}$ = 2.94 g L^{-1}).*

Reactant	Pd activity A_{Pd} [L g^{-1} min^{-1}]
HCB	150
PeCB	2120
1,2,3,4-TeCB	950
1,2,4,5-TeCB	440[a]
1,2,3,5-TeCB	1160
1,2,3-TCB	770
1,2,4-TCB	110[a]
1,3,5-TCB	440
1,2-DCB	2420[b]
1,4-DCB	1060[b]
1,3-DCB	3380[b]
MCB	3210[b]

440 [a] Problems with regard to measurement and reproducibility within the marked experiment, [b] 6 µg L^{-1}

441

442 The specific catalytic activity of the Pd(0) particles for HCB was determined as A_{Pd} =
443 150 L g^{-1} min^{-1}. As a general tendency, for unsaturated substances, an increasing catalytic
444 activity can be observed with decreasing degree of chlorination, which also correlates with
445 increasing water solubility of the chlorobenzenes (Figure S3). However, some of the isomers
446 show a deviation from this general tendency as can be seen for the TCBs in Table 1. As an
447 explanation, the inductive effect can again be considered to affect the reactivity depending on the

448 arrangement of the chlorine atoms. Other studies have already determined the activity of Pd(0)
449 nanoparticles in further dehalogenation reactions. Several experiments were carried out in which
450 halogenated hydrocarbons were degraded by Pd catalysts [27]. Because the type of catalyst
451 particles differed from the ones used in the present study and the particle size was slightly larger,
452 a much lower specific catalyst activity was detected for several substances [27], e.g. for MCB
453 with a catalyst activity of 200 L g^{-1} min^{-1} compared to 3210 L g^{-1} min^{-1} under the here presented
454 conditions. Considering the huge intrinsic Pd activity, the chosen reaction conditions represent a
455 surplus of Pd(0) compared to the low contaminant concentrations, leading to a lower turnover
456 compared to previous studies (e.g., 171 µmol MCB g^{-1} Pd(0) min^{-1} in the present study compared
457 to 35.5 mmol MCB g^{-1} Pd min^{-1} [27]). Different from the conditions in the present study,
458 previous studies on the dechlorination of HCB by Pd used bimetallic or carbon-supported
459 nanoparticles and provided reactant concentrations that have been far above the pollutant's water
460 solubility (e.g., from 0.5 mg HCB L^{-1} in aqueous solution [42] to the g L^{-1} range of HCB
461 provided in organic solvents [28, 43–45]). The small reactant concentrations used in the present
462 study rather refer to relevant aqueous environmental concentrations reflecting the water
463 solubility of reactants (e.g., 6 µg L^{-1} for HCB). The resulting specific activity A_{Pd} given in Table
464 1 can be understood as a material property. Ideally, the catalyst shows its true catalyst activity for
465 a broad contaminant concentration range. Thus, A_{Pd} reflects the volume of contaminated water
466 that can be treated in a certain time frame with a certain amount of Pd, independent of the
467 contaminant concentration as long as there are no negative effects (e.g., catalyst overload by the
468 reactant). After all, the high catalytic activities indicate a relevant potential for the removal of
469 contaminants. However, suspended Pd(0) nanoparticles are known to agglomerate and
470 precipitate quite rapidly, adsorb to the surface of organic matter and are deactivated by a variety

471 of catalyst-poisoning substances [27,46]. Therefore, long-term maintenance of the catalytic
472 performance is challenging. But recent studies have shown that the catalytic activity of
473 nanoparticles is lower but largely retained when embedded in a PDMS coating [23,47,48]. Thus,
474 the high potential of Pd(0) nanoparticles should be further exploited and adjusted to state-of-the-
475 art long-term protection approaches to develop specific applications for environmentally relevant
476 challenges in water treatment.

477

478 **4. Conclusions**

479 The SPME method established for the simultaneous extraction of all chlorobenzenes and
480 benzene in the ng L^{-1} to µg L^{-1} range was shown to be viable for analysis of such substance
481 mixtures comprising a wide span of properties. The dehalogenation reactions in multi-analyte
482 mixtures could be followed much faster than for single components and with high precision
483 using the method presented in this study. For dechlorination of HCB and less chlorinated
484 benzenes by Pd(0) nanoparticles, substitution of vicinal chlorine atoms by hydrogen was
485 confirmed as preferred reaction pathway. Pd(0) nanoparticles showed high catalytic activity
486 allowing treatment of HCB and intermediate products at environmental relevant concentrations
487 with low Pd(0) concentrations in the µg L^{-1} range. Our method allowed to reach permissible
488 concentrations within reaction times as short as one hour which is highly relevant in terms of
489 resource efficiency. However, with regard to the applicability in terms of potential catalyst loss
490 and poisoning, the use of suspended Pd(0) as performed in the present study is not directly
491 transferable to the treatment of contaminated waters. We used this approach to demonstrate the
492 potential to monitor dechlorination experiments by SPME, to allow an in-depth monitoring of

493 reaction pathways, and to provide information on the potential of using Pd(0) for the
494 dechlorination of environmental pollutants. With regard to future applications, Pd(0) particles
495 should be introduced to protective films (e.g., PDMS) in order to prevent catalyst poisoning and
496 loss of Pd. While this results in a reduction of the catalyst activity, it is still seen to be
497 advantageous for environmental applications because the catalyst activity is so high that a certain
498 reduction in activity is outweighed by the benefits of long-term activity protection of the
499 catalysts. The specific Pd activity for the dechlorination of individual chlorobenzenes roughly
500 increased with decreasing chlorination degree. For isomers with the same degree of chlorination,
501 the Pd activity was higher when the inductive effect in the molecules was lower which led to the
502 concept of the inductive effect as kind of shielding wall that limits the accessibility of the
503 nanoparticles and explains the preferred formation of vicinal chlorinated isomers. The concept of
504 the shielding wall can easily be applied to further halogenated compounds and prediction of their
505 hydrodehalogenation behavior.

506

Corresponding Author

* E-mail: Leonard.Boehm@umwelt.uni-giessen.de; phone: +49 641 99 37116; fax: +49 641 99 37109

Funding Sources

This work was conducted in the framework of the "NanoPOP" project ("Mikrobielle Synthese und Recycling von Hybrid Palladium-Nanokatalysatoren und ihre Anwendung für die Behandlung von persistenten Umweltschadstoffen"), funded by the German Federal Ministry of Education and Research (BMBF, FKZ 03X3571).

Acknowledgement

The authors wish to acknowledge financial support of the German Federal Ministry of Education and Research (BMBF) within the project "Mikrobielle Synthese und Recycling von Hybrid Palladium-Nanokatalysatoren und ihre Anwendung für die Behandlung von persistenten Umweltschadstoffen (NanoPOP)", FKZ 03X3571. The authors highly appreciate invaluable contributions by Sylvia Schnell (microbiological expertise and infrastructure provided in the course of the NanoPOP project) and by Jolanta Lyko (technical assistance in the lab).

References

[1] J.L. Barber, A.J. Sweetman, D. van Wijk, K.C. Jones, Hexachlorobenzene in the global environment: emissions, levels, distribution, trends and processes, The Science of the total environment 349 (2005) 1–44.

[2] UNEP, Stockholm Convention on Persistent Organic Pollutants: United Nations Environment Program, 2001.

[3] K. Borgå, G.W. Gabrielsen, J.U. Skaare, Differences in contamination load between pelagic and sympagic invertebrates in the Arctic marginal ice zone: influence of habitat, diet and geography, Mar. Ecol. Prog. Ser. 235 (2002) 157–169.

[4] E.S.C. Kwok, R. Atkinson, Estimation of hydroxyl radical reaction rate constants for gas-phase organic compounds using a structure-reactivity relationship: An update, Atmospheric Environment 29 (1995) 1685–1695.

[5] G.A. Epling, E.M. Florio, Borohydride-enhanced dechlorination of chlorobenzenes and toluenes, J. Chem. Soc., Perkin Trans. 1 (1988) 703.

[6] S. Yamada, Y. Naito, M. Takada, S. Nakai, M. Hosomi, Photodegradation of hexachlorobenzene and theoretical prediction of its degradation pathways using quantum chemical calculation, Chemosphere 70 (2008) 731–736.

[7] J.A. Field, R. Sierra-Alvarez, Microbial degradation of chlorinated benzenes, Biodegradation 19 (2008) 463–480.

[8] P. Xu, G.M. Zeng, D.L. Huang, C.L. Feng, S. Hu, M.H. Zhao, C. Lai, Z. Wei, C. Huang, G.X. Xie, Z.F. Liu, Use of iron oxide nanomaterials in wastewater treatment: a review, The Science of the total environment 424 (2012) 1–10.

[9] H. Hildebrand, K. Mackenzie, F.-D. Kopinke, Highly Active Pd-on-Magnetite Nanocatalysts for Aqueous Phase Hydrodechlorination Reactions, Environ. Sci. Technol. 43 (2009) 3254–3259.

[10] S. De Corte, T. Hennebel, J.P. Fitts, T. Sabbe, V. Bliznuk, S. Verschuere, D. van der Lelie, W. Verstraete, N. Boon, Biosupported bimetallic Pd-Au nanocatalysts for dechlorination of environmental contaminants, Environmental science & technology 45 (2011) 8506–8513.

[11] F.-D. Kopinke, K. Mackenzie, R. Köhler, Catalytic hydrodechlorination of groundwater contaminants in water and in the gas phase using Pd/γ-Al2O3, Applied Catalysis B: Environmental 44 (2003) 15–24.

[12] J. Padmanabhan, R. Parthasarathi, V. Subramanian, P.K. Chattaraj, Molecular structure, reactivity, and toxicity of the complete series of chlorinated benzenes, The journal of physical chemistry. A 109 (2005) 11043–11049.

[13] M. Bunge, K. Mackenzie, Sustainable Synthesis of Palladium(0) Nanocatalysts and their Potential for Organohalogen Compounds Detoxification, in: O.V. Singh (Ed.), Bio-nanoparticles: Biosynthesis and sustainable biotechnological implications, Wiley Blackwell, Hoboken, New Jersey, 2015, pp. 205–224.

[14] B.P. Chaplin, M. Reinhard, W.F. Schneider, C. Schüth, J.R. Shapley, T.J. Strathmann, C.J. Werth, Critical review of Pd-based catalytic treatment of priority contaminants in water, Environmental science & technology 46 (2012) 3655–3670.

[15] M.O. Nutt, J.B. Hughes, S.W. Michael, Designing Pd-on-Au bimetallic nanoparticle catalysts for trichloroethene hydrodechlorination, Environ. Sci. Technol. 39 (2005) 1346–1353.

[16] M. Schlüter, T. Hentzel, C. Suarez, M. Koch, W.G. Lorenz, L. Böhm, R.-A. Düring, K.A. Koinig, M. Bunge, Synthesis of novel palladium(0) nanocatalysts by microorganisms from heavy-metal-influenced high-alpine sites for dehalogenation of polychlorinated dioxins, Chemosphere 117 (2014) 462–470.

[17] B.S. Ballapragada, H.D. Stensel, J.A. Puhakka, J.F. Ferguson, Effect of Hydrogen on Reductive Dechlorination of Chlorinated Ethenes, Environ. Sci. Technol. 31 (1997) 1728–1734.

[18] C.L. Arthur, J. Pawliszyn, Solid phase microextraction with thermal desorption using fused silica optical fibers, Anal. Chem. 62 (1990) 2145–2148.

[19] S. Risticevic, H. Lord, T. Górecki, C.L. Arthur, J. Pawliszyn, Protocol for solid-phase microextraction method development, Nature protocols 5 (2010) 122–139.

[20] H. Piri-Moghadam, F. Ahmadi, J. Pawliszyn, A critical review of solid phase microextraction for analysis of water samples, TrAC Trends in Analytical Chemistry 85 (2016) 133–143.

[21] L. Böhm, R.-A. Düring, H.-J. Bruckert, C. Schlechtriem, Can solid-phase microextraction replace solvent extraction for water analysis in fish bioconcentration studies with highly hydrophobic organic chemicals?, Environmental toxicology and chemistry 36 (2017) 2887–2894.

[22] L. Böhm, C. Schlechtriem, R.-A. Düring, Sorption of Highly Hydrophobic Organic Chemicals to Organic Matter Relevant for Fish Bioconcentration Studies, Environmental science & technology 50 (2016) 8316–8323.

[23] D. Comandella, S. Woszidlo, A. Georgi, F.-D. Kopinke, K. Mackenzie, Efforts for long-term protection of palladium hydrodechlorination catalysts, Applied Catalysis B: Environmental 186 (2016) 204–211.

[24] A.-K. Herrmann, P. Formanek, L. Borchardt, M. Klose, L. Giebeler, J. Eckert, S. Kaskel, N. Gaponik, A. Eychmüller, Multimetallic Aerogels by Template-Free Self-Assembly of Au, Ag, Pt, and Pd Nanoparticles, Chem. Mater. 26 (2014) 1074–1083.

[25] B.G. Oliver, K.D. Bothen, Determination of chlorobenzenes in water by capillary gas chromatography, Anal. Chem. 52 (1980) 2066–2069.

[26] I.M. Chen, F.C. Chang, Y.S. Wang, Correlation of gas chromatographic properties of chlorobenzenes and polychlorinated biphenyls with the occurrence of reductive dechlorination by untamed microorganisms, Chemosphere 45 (2001) 223–229.

[27] K. Mackenzie, H. Frenzel, F.-D. Kopinke, Hydrodehalogenation of halogenated hydrocarbons in water with Pd catalysts: Reaction rates and surface competition, Applied Catalysis B: Environmental 63 (2006) 161–167.

[28] V.A. Yakovlev, V.I. Simagina, S.N. Trukhan, V.A. Likholobov, Kinetic study of liquid-phase hydrodechlorination of hexachlorobenzene on Ni/C and 2%PdNi/C, Kinet Catal 41 (2000) 25–32.

[29] C.A. Coulson, Valence, 2nd ed., Oxford: University Press, London, 1965.

[30] M. Kraus, V. Bazant, Catalysis: Proceedings of the Fifth International Congress on Catalysis, Miami Beach, Fla., 20-26 August (1972) 1073–1083.

[31] S. Arulmozhiraja, M. Morita, Electron Affinities and Reductive Dechlorination of Toxic Polychlorinated Dibenzofurans: A Density Functional Theory Study, The journal of physical chemistry. A 108 (2004) 3499–3508.

[32] H. Fueno, K. Tanaka, S. Sugawa, Theoretical study of the dechlorination reaction pathways of octachlorodibenzo-p-dioxin, Chemosphere 48 (2002) 771–778.

[33] X. Gao, W. Wang, X. Liu, Low-temperature dechlorination of hexachlorobenzene on solid supports and the pathway hypothesis, Chemosphere 71 (2008) 1093–1099.

[34] J.E. Beurskens, C.G. Dekker, H. van den Heuvel, M. Swart, J. de Wolf, J. Dolfing, Dechlorination of chlorinated benzenes by an anaerobic microbial consortium that selectively mediates the thermodynamic most favorable reactions, Environ. Sci. Technol. 28 (1994) 701–706.

[35] J. Dolfing, I. Novak, The Gibbs free energy of formation of halogenated benzenes, benzoates and phenols and their potential role as electron acceptors in anaerobic environments, Biodegradation 26 (2015) 15–27.

[36] Y. Ren, S. Kang, J. Zhu, Mechanochemical degradation of hexachlorobenzene using Mg/Al2O3 as additive, J Mater Cycles Waste Manag 17 (2015) 607–615.

[37] J.L. Howard, Q. Cao, D.L. Browne, Mechanochemistry as an emerging tool for molecular synthesis: what can it offer?, Chemical science 9 (2018) 3080–3094.

[38] S. Agarwal, S.R. Al-Abed, D.D. Dionysiou, E. Graybill, Reactivity of Substituted Chlorines and Ensuing Dechlorination Pathways of Select PCB Congeners with Pd/Mg Bimetallics, Environ. Sci. Technol. 43 (2009) 915–921.

[39] J.-H. Kim, P.G. Tratnyek, Y.-S. Chang, Rapid Dechlorination of Polychlorinated Dibenzo- p -dioxins by Bimetallic and Nanosized Zerovalent Iron, Environ. Sci. Technol. 42 (2008) 4106–4112.

[40] V. Bokare, J.-L. Jung, Y.-Y. Chang, Y.-S. Chang, Reductive dechlorination of octachlorodibenzo-p-dioxin by nanosized zero-valent zinc: modeling of rate kinetics and congener profile, Journal of Hazardous Materials 250-251 (2013) 397–402.

[41] J. Nowak, N.H. Kirsch, W. Hegemann, H.-J. Stan, Total reductive dechlorination of chlorobenzenes to benzene by a methanogenic mixed culture enriched from Saale river sediment, Applied Microbiology and Biotechnology 45 (1996) 700–709.

[42] J. Wan, Z. Li, X. Lu, S. Yuan, Remediation of a hexachlorobenzene-contaminated soil by surfactant-enhanced electrokinetics coupled with microscale Pd/Fe PRB, Journal of Hazardous Materials 184 (2010) 184–190.

[43] V. Simagina, V. Likholobov, G. Bergeret, M.T. Gimenez, A. Renouprez, Catalytic hydrodechlorination of hexachlorobenzene on carbon supported Pd-Ni bimetallic catalysts, Applied Catalysis B: Environmental 40 (2003) 293–304.

[44] Y.-h. Shih, Y.-C. Chen, M.-y. Chen, Y.-t. Tai, C.-P. Tso, Dechlorination of hexachlorobenzene by using nanoscale Fe and nanoscale Pd/Fe bimetallic particles, Colloids and Surfaces A: Physicochemical and Engineering Aspects 332 (2009) 84–89.

[45] S.V. Klokov, E.S. Lokteva, E.V. Golubina, K.I. Maslakov, A.V. Levanov, S.A. Chernyak, V.A. Likholobov, Effective Pd/C catalyst for chlorobenzene and hexachlorobenzene hydrodechlorination by direct pyrolysis of sawdust impregnated with palladium nitrate, Catalysis Communications 77 (2016) 37–41.

[46] N.E. Korte, J.L. Zutman, R.M. Schlosser, L. Liang, B. Gu, Q. Fernando, Field application of palladized iron for the dechlorination of trichloroethene, Waste Management 20 (2000) 687–694.

[47] R. Navon, S. Eldad, K. Mackenzie, F.-D. Kopinke, Protection of palladium catalysts for hydrodechlorination of chlorinated organic compounds in wastewaters, Applied Catalysis B: Environmental 119-120 (2012) 241–247.

[48] D. Comandella, M.H. Ahn, H. Kim, K. Mackenzie, Enhanced protection of PDMS-embedded palladium catalysts by co-embedding of sulphide-scavengers, Science of The Total Environment 601-602 (2017) 658–668.

654 ***Fig. 1.*** *Dechlorination of all chlorobenzenes used as educts. Occurring intermediates with the*
655 *same degree of chlorination are given as the sum of isomers for the sake of clarity. n = 4*
656 *replicates per time step (d50% = 3.9 nm,* $c_{0,CBs}$ *= 3 or 6* $\mu g\ L^{-1}$, c_{Pd} *= 300* $\mu g\ L^{-1}$, c_{NaHCO3} *= 9 g* L^{-1},
658 $c_{Na\text{-}citrate}$ *= 2.94 g* L^{-1}*).*

659

660 ***Fig. 2.*** *Dechlorination of HCB and the formation of intermediate products and benzene over*
661 *time. MCB was not detected. Error bars show sd, n = 4 per time step (Pd with d50% = 3.9 nm,*
662 $c_{0,CBs}$ *= 3 or 6* $\mu g\ L^{-1}$, c_{Pd} *= 300* $\mu g\ L^{-1}$, c_{NaHCO3} *= 9 g* L^{-1}, $c_{Na\text{-}citrate}$ *= 2.94 g* L^{-1}*). The dotted lines*
663 *are added to guide the eye.*

664

665 ***Fig. 3.*** *Dechlorination of HCB using Pd(0) nanoparticles with proposed main stepwise reaction*
666 *pathway (black bold), minor stepwise reaction pathways (black plain), direct reaction pathways*
667 *(grey bold), and not detected reaction pathways (grey dotted).*

668

669 ***Fig. 4.*** *Visualization of inductive effects for the dechlorination of chlorobenzenes.*

670

Figure 1

Click here to download high resolution image

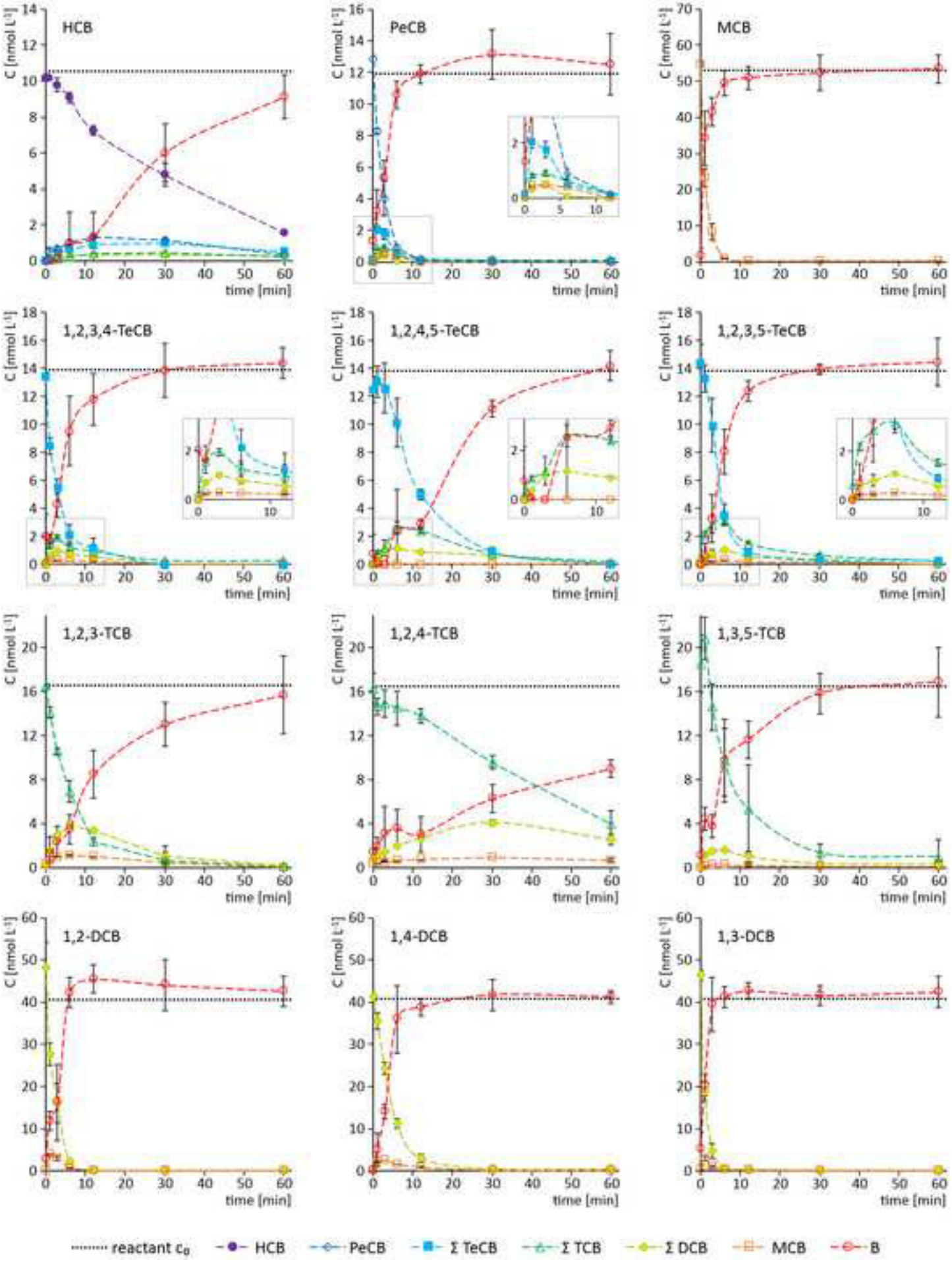

Figure 2

Click here to download high resolution image

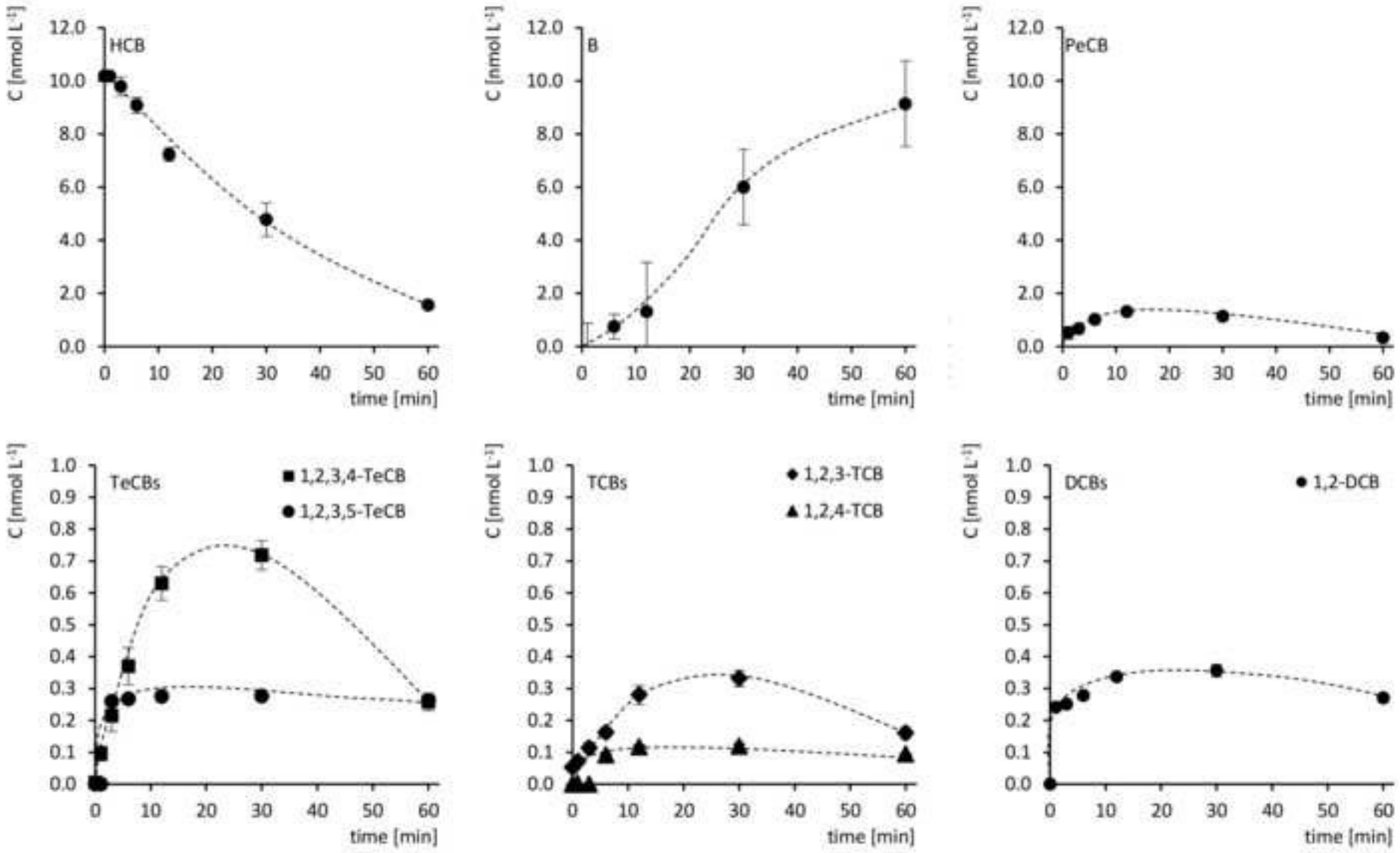

Figure 3
Click here to download high resolution image

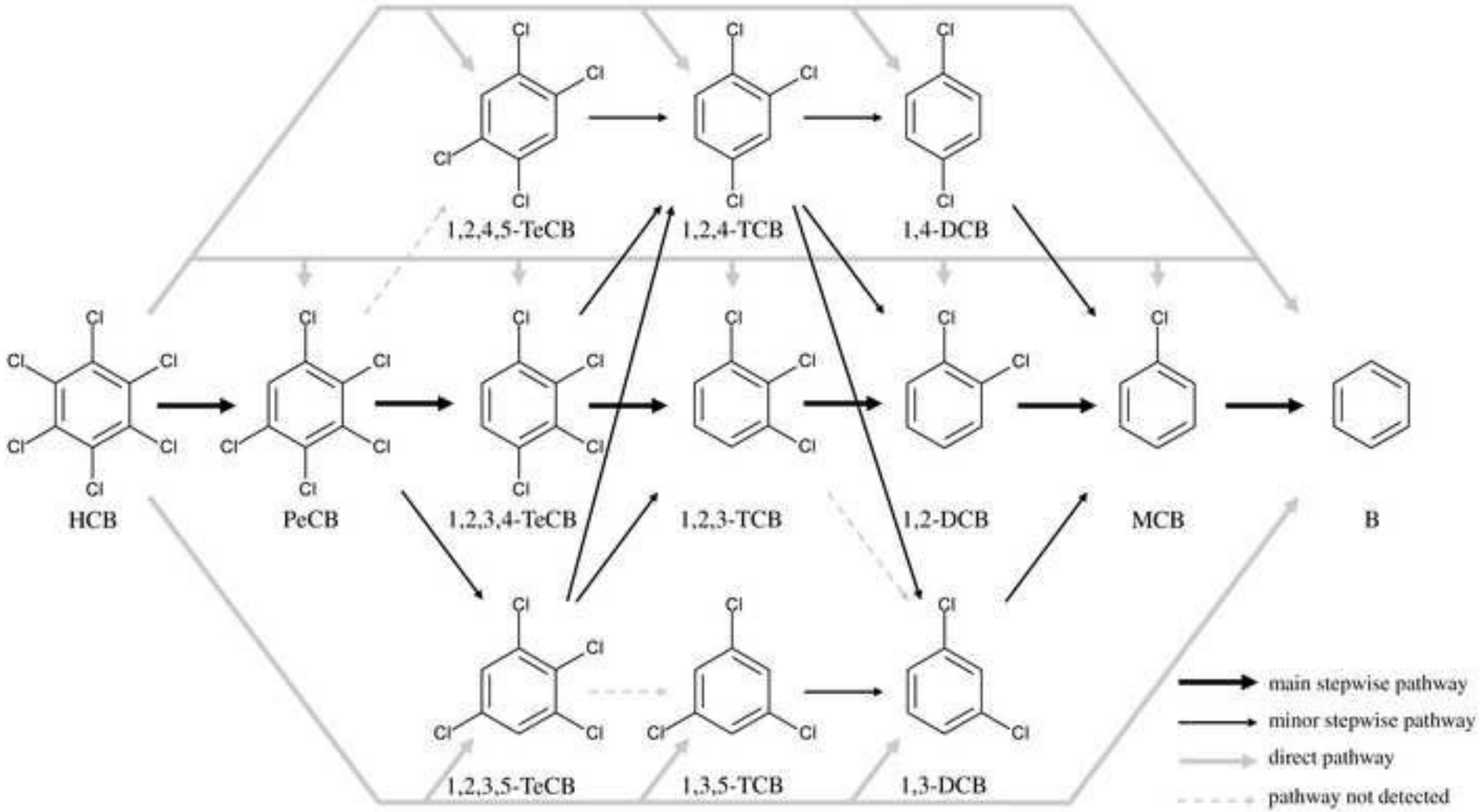

Figure 4

Click here to download high resolution image

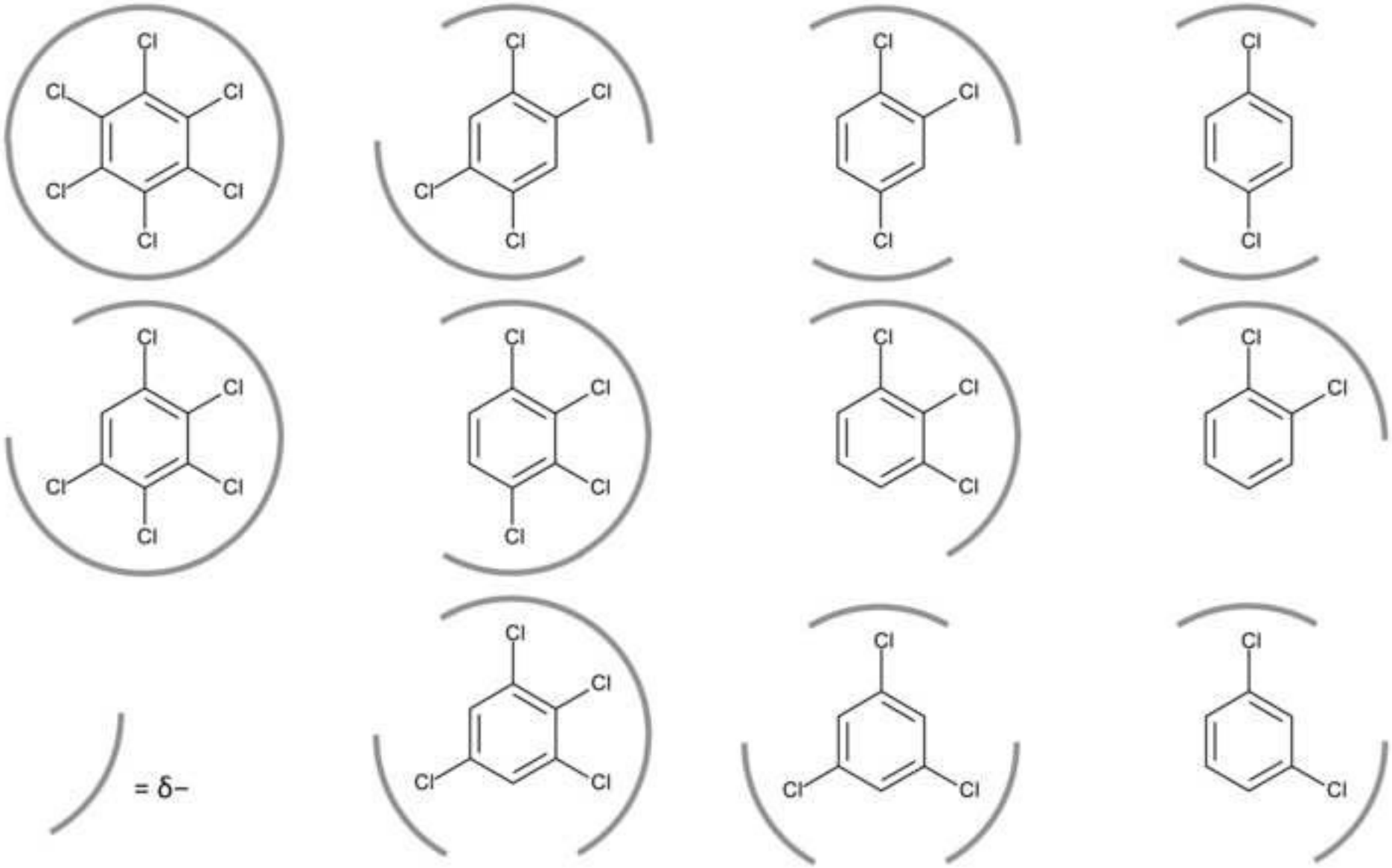

*Graphical Abstract